Temporal Microbial Community Dynamics within a Unique Acid Saline Lake

Noor-ul-Huda Ghori[1,2*], Michael. J. Wise [2,3], Andrew. S. Whiteley[1]

[1]Microbial molecular and ecology group, The School of Agriculture and Environment (SAgE), The University of Western Australia, Perth, WA, Australia

[2]The Marshall Centre, The School of Biomedical Sciences, The University of Western Australia, Perth, WA, Australia

[3]The School of Computer Sciences and Engineering, The University of Western Australia, Perth, WA, Australia

*** Correspondence:**

Corresponding Author

Noor-Ul-Huda Ghori

noor-ul-huda.ghori@uwa.edu.au

Keywords: Polyextremophile$_1$, 16S rRNA$_2$, 18S rRNA$_3$, Temporal microbial dynamics$_4$, Acid Saline$_5$.

Abstract

Lake Magic is one of the acidic hypersaline lakes (ca. 1 km in diameter) present within the Yilgarn Craton in WA**.** This unique lake exhibits extremely low pH (<1.6) coupled to very high salinity (32% TDS) with the highest concentration of aluminium (1774 mg/L) and silica (510 mg/L) in the world. Previous studies on Lake Magic diversity has revealed that the lake hosts acidophilic, acidotolerant, halophilic and halotolerant bacterial species. These studies provide indicators of the population residing within the lake. However, they do not emphasize the survival mechanisms adopted by the resident microorganisms and how the diversity of microbial populations residing within the lake changes during the dynamic stages of flooding, evapo-concentration and desiccation. We have studied the bacterial and fungal diversity in Lake Magic via amplicon sequencing and functional analysis through different stages of the lake in a span of one year, in the salt and sediment layer. Our results highlight that the diversity in Lake Magic is strongly driven by the pH and salt concentrations at different stages of the lake. The microbial community becomes more specialised in specific functions during more extreme stages. This also suggests that microbial interactions are involved in stabilising the ecosystem and is responsible for the resistance and resilience of these communities as the interactions of these microbes create a safe haven for other microbes to survive during more extreme stages.

1 Introduction

Acid saline lakes represent one of the most extreme aquatic environments on Earth. They are poly-extreme ecosystems, exhibiting extremely acidic pH and salinities close to saturation. Such environments are of significant microbial interest as they host organisms that are not only capable of withstanding pH and salinity stress, but also survive in the presence of additional stressors such as high metal concentrations and low nutrients (Mormile *et al.*, 2007; Heidelberg *et al.*, 2013; Johnson *et al.,* 2015; Zaikova *et al.*, 2018). Moreover, they serve as a reservoir of novel microbial functions, such as acidophilic microorganisms that have been used for extracting metal ores from sulphide minerals. Hence, such environments are of significant interest to scientists interested in understanding the fundamental concepts of microbial mechanisms used to cope with significant stressors, as well as applied areas developing microbial consortia for bioprocessing applications (Dopson *et al.*, 2017).

Lake Magic is one of the acidic hypersaline lakes (ca. 1 km in diameter) present within the Yilgarn Craton in WA**.** This unique lake exhibits extremely low pH (<1.6) coupled to very high salinity (32% TDS) with the highest concentration of aluminum (1774 mg/L) and silica (510 mg/L) in the world (Bowen and Benison 2009; Conner and Benison, 2013). Lake Magic, similar to other lakes in WA, has dynamic and characteristic stages of lake transformation, including flooding, evapo-concentration and desiccation that are driven by the local seasons (Bowen and Benison 2009; Conner and Benison, 2013). The lake is fed via both regional acidic groundwater and infrequent precipitation (Benison *et al.*, 2007). Recent studies of the microbial diversity of Lake Magic has revealed that the lake hosts acidophilic, acidotolerant, halophilic and halotolerant bacterial species (Zaikova *et al.,* 2018). Moreover, fluid inclusions of halite crystals from Lake Magic, exhibited the presence of micro-algae and prokaryotes trapped within them (Conner and Benison, 2013). More recently, metagenomic analyses of lake water, groundwater and within the sediment of Lake Magic revealed that the lake is dominated by only a few

species, such as *Salinisphaera*, and has a low representation of other bacterial species (Zaikova *et al.,* 2018). Interestingly, the pelagic zone of the lake was abundant in eukaryotes, including fungi and green algae, giving rise to the bright yellow colour of the lake (Zaikova *et al.,* 2018, Conner and Benison, 2013). These studies provide indicators of the population residing within the lake and the functional niches they occupy. However, they do not emphasize the survival mechanisms adopted by the resident microorganisms and how the diversity of microbial populations residing within the lake changes during different transformational stages of the lake.

Molecular approaches to understand the dynamics of Yilgarn Craton lakes in the past have focused primarily on spatial composition (Mormile *et al.*, 2009; Johnson *et al.*, 2015; Zaikova *et al.*, 2018; Aerts *et al.*, 2019). However, these studies implicitly assume that a single time point can provide a comprehensive representation of the community members. In opposition, temporal approaches to study microbial community dynamics have recently revealed considerable variability within microbial community compositions over time (Ju and Zhang, 2014; Chénard *et al.*, 2017; Nagarkar *et al.*, 2018; Cruaud *et al.*, 2019), showing that some taxa remain consistent in their abundance whilst others exhibit sudden blooms (Nagarkar *et al.,* 2018).

We hypothesize that the large fluctuations in environmental parameters during lake transformations are key drivers which will lead to marked changes in microbial populations, and contribute to the mechanisms driving the dynamics of these communities (Cruaud *et al.,* 2019). Therefore, studying the temporal dynamics of microbial communities in poly-extreme ecosystems such as Lake Magic could reveal crucial information about the trophic interactions and survival mechanisms (Nagarkar *et al.*, 2018). This study attempts to investigate the diversity and functional dynamics of bacterial, archaeal (referenced as 'bacterial' from hereon) and fungal communities, over a period of one year. Using 16S rRNA gene and ITS gene sequencing data, we elucidate the diversity patterns generated during lake

transformations and assess likely mechanisms the resident microorganisms adopt in order to survive in the face of multiple stressors.

2 Materials and Methods

2.1 Sample collection

Samples were collected from Lake Magic for every lake stage in a span of one year (July 2017-July 2018). Multiple sampling sites were chosen around the lake to eradicate a spatial sampling effect. Sediment samples were taken as cores, which were divided into salt mat and sediment layers (**Figure 1)**. All samples were taken with sterile cores and spatulas. After every sample the cores and spatulas were sterilized with 70% ethanol. A total of 40 sediment samples and 40 salt mat samples (8 cores for each time point) were collected. Temperature, pH, and salinity were measured for each sampling point. All samples were kept frozen at -20°C in 50 ml Falcon tubes until further processing.

2.2 DNA extraction, PCR and amplicon sequencing

DNA from sediment and salt mat samples was extracted using a method developed for acid saline sediments. Briefly, 0.4g sediment sample in 2ml tubes containing glass beads. To this 900µl of extraction buffer (consisting of 0.2M sodium phosphate buffer, 0.2% CTAB, 0.1M NaCl and 50mM EDTA), 100 µl of 10% SDS and 10 µl of Proteinase K (20 mg/ml). The mixture was kept at -80C for 5 min and then heated at 70C for 20 min. The mixture was subjected to mechanical agitation at 20Hz for 20min after which the tubes were kept on ice for 5 min. The mixture was centrifuged at 10, 000 x g for 5 min. To the supernatant 750 µl of chilled phenol-chloroform-isoamyl (pH 8) solution was added and centrifuged for 20 min at 10, 000 x g. Aqueous layer was transferred to sterile tube and 600 µl of

chilled chloroform -isoamyl (pH 8) solution was added. The mixture was centrifuged at 10, 000 x g for 5 min. Next, to the aqueous layer 650 µl of 20% PEG, 2.5 M NaCl was added and incubated at 4C for overnight. The solution was centrifuged for 20 min at 10, 000 x g. The obtained pellet was washed with 70% ice cold ethanol and 2 µl glycogen. The final pellet was dissolved in 50 µl of TE buffer. All extractions were carried out in triplicate. Tubes containing no sample were incorporated as extraction blanks (controls) and were treated identical to sample extractions. DNA concentration was measured through fluorometry using a Qubit dsDNA HS Assay Kit with a Qubit 2.0 fluorometer (Life Technologies).

Extracted DNA from all timepoints were diluted 10-fold prior to PCR amplification of the 16S rRNA and ITS genes. All PCR reactions were carried out in triplicate. PCR amplification of the 16S rRNA gene V4-V5 region was performed using the universal PCR primer set 515F and 806R, targeting members within both bacterial and archaeal domains (16). The forward primer included the addition of an Ion Torrent PGM sequencing adapter, a GT spacer and a unique Golay barcode to facilitate multiplexed sequencing. Barcoded PCR reaction mixtures (20 µl) consisted of DNA template (1 µl), universal primer mix (untagged 515F and 806R at a final concentration of 0.2µM), tagged 515F primer (0.2 µM), 600 ng BSA (Life technologies) and 2.5 x 5'Hot Master Mix (5Primer, Australia). The PCR cycle was set at 94C for 2min followed by 25 cycles of 94 min for 45 sec, 50C for 60 sec and 65C for 90. This was followed by 2 cycles of 94C for 45 sec, 65C for 90 sec and final extension at 65C for 10 min.

Amplification of the fungal component was carried out using the universal primer set ITS1 F and ITS2 R, with the addition of an Ion Torrent PGM sequencing adapter, a GT spacer and a unique Golay

barcode to the forward primer. The barcoded PCR primer mixtures (20 µl) included DNA template (1 µl), universal primer mix (untagged ITS1 F and ITS2 R at a final concentration of 0.2 µM), 600 ng BSA (Life technologies), tagged ITS1 F primer (0.2 µM) and 2.5x 5' Hot Master Mix (5Primer, Australia). The PCR conditions included initial denaturation at 94 for 2 min followed by 25 cycles of 94C for 45 sec, 50C for 60 sec and 65C for 90 sec. This was followed by 9 cycles of 94C for 45 sec, 65C for 90 sec and 65 for 10 min.

Several positive, no template (as negative controls) controls and DNA extraction controls (extraction blanks) were amplified along with the samples for both bacterial and fungal marker genes. PCR reaction performance was checked by loading PCR amplicons along with positive and negative controls on a 2% (w/v) agarose gel. The amplicons were quantified using a Qubit dsDNA HS Assay Kit on the Qubit 2.0 fluorometer (Life Technologies). All amplicons were subsequently pooled in one composite mixture at a concentration of 20 ng/µl, including negative controls. The pool was purified using AMPure XP (Beckman Coulter, Australia) and the quality of the pool was checked by visualizing on a 2% (w/v) agarose gel. The composite pool was sequenced on an Ion Torrent PGM.

2.3 Sequence analysis and statistical analysis

Raw sequences were de-multiplexed and quality filtered through a custom QIIME pipeline (Quantitative Insights into Microbial Ecology) (Caporaso *et al.,* 2010) with a minimum average quality score of 20. The minimum sequence length was maintained at 130 b.p. and maximum sequence length of 350 b.p. Chimeric sequences were removed using USEARCH v6.1. No forward or reverse primer mismatches or barcode errors were allowed and maximum sequence homopolymers allowed were 15.

153 The maximum number of ambiguous bases was set at six. Denovo OTU picking was performed using
154 ULCUST at 97% sequence identity cut off values and taxonomy was assigned through the Greengenes
155 database (version 13.8). For fungal data, taxonomy was assigned using the SILVA v123 database
156 (Quast *et al.*, 2012).
157
158 The OTU tables obtained for different levels of taxonomy were used as measures of taxa relative
159 abundance in univariate statistical analysis. The OTUs detected in negative controls were manually
160 removed from the data set. Alpha (α)- diversity at the phylum level for both 16S rRNA gene and ITS
161 gene data was calculated using the richness, evenness and Shannon Weiner diversity index using the
162 relative frequency table generated from a rarefied 'biom' table**.** Data normality was checked with the
163 Shapiro-Wilk test and log transformations of the data were performed where appropriate. Differences
164 in the diversity for each stage and layer (sediment, salt mat), was calculated using a two-way analysis
165 of variance (ANOVA). Tukey HSD *post hoc* comparisons of groups were used to identify which groups
166 were significantly different from each other.
167
168 Beta diversity (β) of microbial communities was calculated with nonmetric multidimensional scaling
169 (nMDS) using Bray-Curtis dissimilarity (Bray and Curtis, 1957). Statistical significances of
170 dissimilarity, based on temporal data and sample layer, was assessed using main effect and pairwise
171 ANOSIM in R using the vegan package.
172
173 Phylogeny was inferred using Phylosift (Darling *et al*., 2014) for sequences that could not be classified
174 past the domain level. The OTU abundance and diversity patterns were calculated using the vegan
175 package (Dixon, 2003) in R software (R Core Team, 2014). Plots and heat maps were produced using
176 'ggplot2' (Wickham, 2011), 'ggpubr' packages in R and the online suite 'Calypso' (Zakrzewski *et al.*,
177 2017).

Predicted microbial functions of the bacteria residing within Lake Magic were generated using FAPROTAX, using default settings. FAPROTAX is a manually constructed database that maps the microbial taxa to metabolic functions (Louca *et al.,* 2016). The output from FAPROTAX was visualised in R using the ggplot2 package.

2.4 Chemical analysis

Ten grams of sediment sample for each time point was oven dried at 60ºC until completely desiccated. The sample was crushed, sieved, packed in plastic bags and sent to the School of Agriculture and Environment (SAgE), University of Western Australia (UWA) chemical analysis laboratory. The analytical analysis included analysis of phosphorus, potassium, sulfur, organic carbon, nitrogen, iron, copper, sodium, boron, calcium, zinc, aluminum, magnesium and manganese. Concentrations were expressed as percentage per weight and mg/kg.

3. Results

3.1 Lake stages and physico-chemical parameters

A total of 5 time points representing 5 different stages of Lake Magic were sampled for this study. Although the lake did not go through some of the more extreme physical changes during the year, the transformation of one stage to the next was evident. Namely, we observed flooding, early evapo-concentration, mid evapo-concentration, late evapo-concentration and early flooding in the lake **(Figure 2)** details of which are presented in **Table 1** and **Table 2.** During the span of this study the lake did not reach complete desiccation due to heavy rainfall from 2017 to 2018.

The first sampling point was during late winter to early summer in 2017, where the lake was filled with several centimeters of clear blue water (July 2017) **(Figure 2A)**. The lake sediment was rich in clay

and a small amount of wet salt mat sample was acquired. In October 2017, the lake became shallower **(Figure 2B)** during early evapo-concentration **(Table 1),** characterized by clear water but where halite precipitation was evident on the lake shore. The lake transformed into a shallow yellow lake during January 2018 sampling **(Figure 2C)** where the surroundings of the lake were rich in halite precipitation, the lake itself exhibited a pungent acidic odour and the salt mat became desiccated and substantial. During mid-summer (March 2018) the lake bed became dry and a thick salt crust was observed on the surface of the sediment **(Figure 2D)** with visible salt crystals **(Figure 1),** constituting the late evapo-concentration stage. At this stage the lake was also rich in iron oxide precipitation, which was evident due to its distinct colour. The final sampling timepoint was the beginning of the flooding stage in July 2018 **(Figure 2E)** where the lake started to fill with water, with a concomitant dissolving of the halite and iron precipitation observed during the evapo-concentration stages. The chemical data has been summarized in **Table 2.**

3.2 Temporal dynamics of the Lake Magic microbiome

In order to assess the microbial community dynamics in the lake at different stages, we used 16S rRNA gene and ITS gene Ion Torrent sequencing (15 Salt mats; 15 Sediments) in triplicate. After DNA extraction, all samples had detectable amounts of DNA, but the DNA concentration was consistently higher for salt mat samples when compared to the sediment samples. However, there was no significant difference (ANOVA $p>0.05$) between diversity and richness indices of salt mat and sediment layers for both bacteria and fungi analyses **(Supplementary Figure 1),** likely indicating minimal diversity analysis bias despite wide variations in DNA extraction concentrations. Generally, we found DNA extraction easier from salt mat samples, relative to sediment samples, due to the lower amount of clay present in the salt mat samples.

A total of 330,913 reads were obtained for 16S rRNA microbiome analyses, representing 15947 OTUs. The OTUs were assigned to 37 phyla, 135 classes, 260 orders, 426 families and 739 genera of archaea and bacteria. Only OTUs which appeared in sequenced negative controls were discounted from the analyses and no other OTUs were filtered. This is because low abundance OTUs can have a significant effect on the diversity metrics for the microbial communities in low biomass environments, hence, filtering of OTUs with low representation in the microbiome can result in loss of crucial information. Analysis of the ITS gene sequences revealed a total of 724,490 reads, representing 4005 OTUs and were assigned to 15 phyla, 44 classes, 86 order, 177 family and 259 genera.

3.3 Bacterial communities are dynamic in Lake Magic

The Lake Magic microbiome OTU richness was analyzed for salt mat and sediment samples **(Figure 3A)** at phylum level which varied significantly between the five stages of the lake (ANOVA p= 0.001). The richness index varied from 9 to 23 for 16S rRNA gene and the OTU richness was significantly higher during the EF stage (mean richness = 21). The second highest OTU richness was observed during the ME stage (mean richness = 18). The LE stage showed the lowest mean richness of 13.6, whereas, OTU richness at the FL stage was significantly different and showed a mean richness of 16. A mean richness of 15.5 was seen during EE stage.

The Lake Magic microbiome diversity varied during the different lake stages **(Figure 3B)** and followed a similar trend to that of OTU richness. The Shannon diversity index ranged from 1.61 to 2.13 for bacterial communities, where the diversity was seen to increase during EE (mean diversity = 1.65) and the ME stage (mean diversity =1.87). However, the diversity decreased during the LE stage and was recorded as the lowest diversity index (mean diversity= 1.39) of all stages. The highest diversity was seen during the EF stage (mean diversity= 2.11). The ANOVA test was further analyzed with a *Tuckey post hoc* test for diversity and richness indices, which revealed that the diversity during FL, LE and EF

stages were significantly different from each other, whereas, the richness was significantly different only during FL and EF stages.

The Lake Magic bacterial composition under different lake stages was analyzed and are shown in (**Supplementary Figure 2).** Archaeal community diversity in the microbiome was represented by only two phyla, the *Crenarchaeota* and the *Euryarchaeota,* whilst the bacterial domain contributed the dominant microbial sequences observed within the 16S rRNA gene analyse**s.** The majority of the sequences for bacteria originated from two phyla: *Bacteriodetes* (20%) and *Proteobacteria* (39%), most of which could not be classified below family level, indicating that a large proportion of the bacterial taxa in Lake Magic appear to be relatively poorly characterized.

3.4 The bacterial community becomes more specialized as stress increases

For taxa which could be classified to genera, varying trends were observed during different lake stages and within the sample layers **(Supplementary Figure 3)**. Specifically, key bacterial genera fluctuated within the salt mat and sediment during the various lake stages. The correlation analysis of chemical data with the bacterial diversity revealed that microbial dynamics is strongly driven by salinity, temperature, pH and carbon content in the lake **(Supplementary Figure 4)**. For instance, members of the *Acidiphilium* genus were low in abundance during the FL stage in both the salt mat and sediment samples, whilst their relative abundance was seen to increase within in the salt mat during evapo-concentration stage as the lake conditions became more stressful. A significant increase (ANOVA, $p<0.05$) in *Acidiphilium* relative abundance was observed within the salt mat during the LE stage and significantly decreased during the EF stage of the lake **(Supplementary Figure 3, *Acidiphilium*)**. Similarly, the *Acidobacterium* genus' relative abundance was high within sediment during the FL stage and a significant increase in abundance within the salt mat was seen during all evapo-concentration stages **(Supplementary Figure 3, *Acidobacterium*)**. Similar to the *Acidiphilium, Acidobacterium*

abundance decreased when the lake was in the EF stage. In contrast, sequences belonging to the *Arthrobacter, Bacillus, Flavbacterium and Sporosarcina* genera increased significantly in abundance during the EF stage in both the sediment and salt mat, whilst genera such as *Nitrososphaera* were only present during the EF stage in high abundance.

Interestingly, it was also observed that the abundance of the *Sulfurimonas, Syntrophobacter, Halothiobacillus, Acidobacterium, Acidiphilium and Alicyclobacillus* genera decreased during the EF stage in both the salt mat and the sediment whilst, the *Syntrophobacter* population increased in relative abundance within the sediment during LE. During the FL stage *Salinisphaera* was found to be more abundant in the salt mat when compared to the sediment. However, when compared to the LE, its abundance increased in the salt mat **(Supplementary Figure 3).** Overall, from these data it was evident that the sediment becomes more dominated by bacteria that were not specialized for surviving in the environmental conditions, whereas, the salt mat became dominated with specialized microbes such as *Salinisphaera* and *Acidobacterium*.

3.5 The fungal community becomes less diverse under extreme conditions within Lake Magic

The diversity and richness of the fungal community within Lake Magic significantly decreased (ANOVA, $p < 0.001$) as the lake conditions became more extreme. The richness index ranged from 2 to 7 whereas the Shannon diversity index ranged from 0.004 to 1.28 **(Figure 4A and 4B).** The highest mean richness was observed for the FL and EE stage. The OTU richness consistently decreased after the EE stage, with lowest OTU richness observed for the EF stage (mean richness = 2). The fungal diversity showed a varying trend when compared to OTU richness, where the highest diversity index was observed for the FL stage (mean diversity index =1.11) whereas the lowest was observed for the extreme EF stage (mean diversity index= 0.28). A *Tuckey post hoc* test revealed that the FL and EE stage were statistically similar to each other, whilst, the ME and LE stages were statistically similar,

and the EF stage was significantly different from all other stages. Additionally, a *Tuckey* test for OTU richness showed that the FL, EE and EF stages were significantly different from all other stages.

Interestingly, when the fungal community composition was visualized **(Supplementary Figure 5)**, an increase in unidentified fungi belonging to the Ascomycota phylum was observed. This indicated that a large portion of the fungi living in Lake Magic are likely unidentified. The salt mat during the EF stage was, however, seen to be the most diverse when compared to other time points and was abundant with the *Cladosporium* genus. Variation in the composition of other genera including *Fusarium, Ulocladium* and *Hostaea* was also seen.

3.6 Beta diversity of the bacterial and fungal communities

The dissimilarity between microbial communities at different lake stages was assessed using Nonmetric multidimensional scaling (nMDS) and Bray-Curtis dissimilarity indices. The sediment and salt mat bacterial communities from the FL, ME, LE and EF stages tightly clustered together **(Figure 5A)**. In contrast, the salt mat and sediment communities under the EE stage clustered separately (ANOSIM, R^2= 0.49, p=0.001). However, similar to alpha diversity, when an ANOSIM test was applied to determine the variability in the salt mat and sediment samples no significant difference was observed.

The nMDS analysis of fungal communities showed less clustering when compared to the bacterial community analysis **(Figure 5B),** where none of the lake stages clustered separately. This indicated that the members identified within the *Ascomycota* phylum vary for different lake stages (ANOSIM, R^2 =0.462, p= 0.001), but no significant difference was seen between sediments or salt mat samples.

3.7 Predicted ecological functions of the bacterial communities

The ecological function of the bacterial communities analyzed was predicted using the FAPROTAX pipeline for the different stages of the lake. These analyses indicated aerobic chemoheterotrophy, iron oxidation and sulphur related pathways as likely dominant functions within the lake's bacterial community **(Figure 6)**. Functions related to carbon metabolism, such as methylotrophy and methanotrophy, were predicted but were not abundant. Nitrogen related functions included nitrification and ammonia oxidation and were observed to fluctuate between different lake stages. For instance, these data indicated that nitrification and ammonia oxidation were significantly higher within the salt mat during the EF stage **(Supplementary Figure 6)**. Interestingly, the nitrogen related activity was also high in the sediment samples during the EE and ME lake stage. Sulphur related functions were lower during the EF stage, but significantly increased in the sediment layer during all evapo-concentration stages. Sulphur related activity was found to be highest in the sediment during the EE stage. Iron oxidation and reduction was relatively low at all timepoints, but significantly increased during the EE and LE stage within the sediment layer. Finally, Iron based respiration pathways fluctuated more frequently when compared to sulphur and nitrogen related functions during all lake stages **(Supplementary Figure 6)**.

4. Discussion

Acid saline lakes in WA host unique microorganisms that can be studied to understand life under extreme conditions, novel biogeochemical processes and new biotechnological avenues (Benison *et al*., 2007). In this chapter, the bacterial and fungal microbial community dynamics were studied using a temporal approach to resolve how an extreme lake microbiome changes during different stress phases due to changes in the physico-chemical properties of the habitat.

Previous studies on acidic hypersaline lakes in WA revealed a high level of bacterial diversity within Lake Magic and other WA lakes water (Mormile *et al.,* 2009; Zaikova *et al.*, 2018), but have relied upon single time (lake stage) sampling points. Our results indicate that the alpha (α)-diversity of the bacterial and fungal microbial communities differed significantly between the less extreme (FL) stage and the more extreme (LE) stage. These differences indicated that the lake microbiome diversity is driven to a large degree by the high salt and low pH conditions within the lake (Podell *et al.,* 2014). It has previously been reported for hypersaline environments that the ionic concentration in these environments hinders the solubility of oxygen, and hence, the oxygen concentration is very low in acid saline lakes (Sherwood *et al.,* 1991). However, the majority of microorganisms isolated from hypersaline environments are aerobic heterotrophs who are capable of anaerobic facultative fermentation (Dyall-smith, 2009). Our results are also in line with these previous findings. Moreover, our results show that the number of OTUs in the salt mat layer were consistently higher in all samples. These results are also similar to the results obtained by Aerts *et al.*, (2019), for four acid saline lakes in Western Australia, and suggest that the majority of the microbial community diversity resides in the salt mat, where it likely has increased access to light, water and oxygen. This is likely explained by the availability of oxygen at the air/water interface, which exhibits an unequal distribution of oxygen between the salt mat and the sediment layer. Since the salt mat is directly in contact with the water column in the lake there is higher availability of oxygen locally (Podell *et al.,* 2014). Comparing the microbial composition of the salt mat and sediments in Lake Magic also indicates that microorganisms more tolerant to high salt and pH conditions are selected within the salt mat, where the conditions are harsher than those in the sediment.

The prokaryotic community at all stages of the lake cycle was dominated by halotolerant and acidophilic microorganisms, whilst archaeal taxa were found in much lower abundances. Archaeal sequences were derived from only two phyla and these observations are in good agreement with

375 Johnson *et al.,* (2015) who observed low archaeal diversity within four acidic hypersaline lakes in
376 Yilgarn Craton. It has been reported for Lake Tyrell in Victoria, Australia, that succession of different
377 microorganisms is dependent upon the solutes present in the lakes (Podell *et al.,* 2014). Hence, the
378 variation in solute concentration in Lake Magic at different stages is likely driving the succession of
379 archaea and bacteria. It could also be hypothesised that bacterial taxa outcompete archaeal taxa in these
380 unique environments because of the dynamic nature of the WA lakes, where environmental changes
381 are frequent and, therefore, stress tolerant species are selected, as opposed to obligate archaeal
382 extremophiles (Benison and Bowen, 2006).
383
384 Organic carbon and nitrogen values were found to be low at all lake stages and increased slightly during
385 the flooded (FL) stages, in line with previous studies in similar lakes in WA (Ruecker *et al.,* 2016;
386 Aerts *et al.*, 2019). Similarly, phosphorus levels were also low in Lake Magic, as in other WA lakes
387 (Aerts *et al.*, 2019), with phosphorus often being considered a limiting factor along with carbon and
388 nitrogen for the growth of microorganisms (Elser *et al.,* 2007). Microbiome community analyses
389 indicated an abundant community of heterotrophs within the lake and hence, low carbon, nitrogen and
390 phosphorus are likely to be responsible for the low the biomass in these samples (Aerts *et al.*, 2019).
391 However, carbon and nitrogen levels were highest during the ME and these increases are likely due to
392 photosynthetic inputs via blooming of the saline tolerant algae *Dunaliella.* This is also reflected in the
393 increased microbial diversity during the ME stage. Blooming of algae commonly occurs during this
394 lake stage and provides a source of photosynthetically derived nutrient input which causes increased
395 diversity in the lake (Zaikova *et al*., 2018).
396
397 During the evapo-concentration stages iron concentrations increased which was also mirrored in the
398 predicted microbiome functions of increased iron respiration activity within the bacterial community.
399 Iron metabolism is considered an important function of the sediment inhabitants and is thought to be

responsible for the lowering of pH in the sediment (Lu *et al.*, 2016; Zaikova *et al.*, 2018). The *Alicyclobacillus* genus members are reported to be involved in iron oxidation along with archaea in other acid saline lakes in WA (Johnson *et al.*, 2015; Lu *et al.*, 2016). The members of the genus are also capable of reducing iron (Yahya *et al.,* 2008; Lu *et al.*, 2010). Previous metagenomic studies of Lake magic indicated that *Alicyclobacillus* was the most abundant genus within the sediment. Moreover, the *Acidiphilium* genus was also found to be abundant in the sediment samples (Zaikova *et al.,* 2018) with members of this genus are involved in iron reduction (Weber *et al.,* 2006; Sánchez-Andrea *et al.*, 2011; Zaikova *et al.*, 2018).

These data indicated, that the abundance of the *Alicyclobacillus* and *Acidiphilium* genera varied across different lake stages and is likely more complicated than first thought, in terms of lake biogeochemistry (Zaikova *et al.,* 2018). *Alicyclobacillus* abundance was significantly higher in sediment samples during the FL stage and was significantly increased during the EE stage within the salt mat samples. In contrast the, *Acidiphilium* genus was more abundant within the salt mat samples during the later LE stage. Interestingly the overall abundance of these genera decreased during the higher stress stages of the lake. Previously it has been suggested that archaea dominate iron oxidation in acid saline extreme environment and that the role of bacteria is limited. Moreover, the Iron activity is known to decrease by the presence of high salt in the environment (Lu *et al.,* 2016). In the study, *Acidiphilium* spp. were isolated from an acid saline lake in WA which formed long filamentous structures during low pH and high salinity conditions indicating that these species have developed a coping mechanism for extreme stress (Lu *et al.,* 2016). Examining the functional profile of our samples it can be seen that predicted iron respiration would increase significantly in the sediment during the EE and LE stage and is the lowest in the sediment during the FL stage potentially because of the coping mechanism adapted by these species.

425 The activity of acidophiles is known to decrease significantly in presence of high concentration of
426 chloride ions (Suzuki *et al.*, 1999; Shiers *et al.*, 2005). However, Lu *et al.,* (2016) found that
427 *Acidiphilium* spp. formed long filaments as a coping mechanism to high chloride ions within the
428 Dalyup river in WA. These data, in concert with previous results, suggest that iron metabolism is
429 affected by the presence of chloride ions and we hypothesise that this may explain the bacterial spp. of
430 *Alicyclobacillus* and *Acidiphilium* being dominant during EE and FL stages. These data also suggest
431 that under the high chloride conditions, based upon community data, these species are responsible of
432 lowering the pH in the sediment. Hence, we postulate from these results that microorganisms in Lake
433 Magic adapt to stressful conditions of pH and salinity not only physiologically, but also play crucial
434 roles in changing their external environment making it more habitable for themselves and other
435 members of the Lake.
436
437 One of the most abundant genera detected in these data was the *Salinisphaera* (7%), in both the
438 sediment and salt mat. *Salinisphaera* species are mesophilic, halotolerant and slightly acidophilic (pH
439 range 5.0-7.5), surviving in a range of moderately acidic and saline conditions as well as high
440 concentrations of metal ions. Species belonging to the *Salinisphaera* genus have been isolated from a
441 range of environments, including hydrothermal vents, solar salterns, brine from salt wells, seawater
442 and marine fish surfaces (Antunes *et al.*, 2003; Mormile *et al.*, 2007; Crespo-Medina *et al.*, 2009; Bae
443 *et al.*, 2010; Gi *et al.*, 2010; Park *et al.*, 2012; Zhang *et al.*, 2012; Shimane *et al.*, 2013). Critically,
444 these species are able to metabolize both autotrophically and heterotrophically (Antunes *et al.,* 2003;
445 Crespo-Medina *et al.*, 2009; Bae *et al.*, 2010; Antunes *et al.*, 2011a; Park *et al.*, 2012; Zhang *et al.*,
446 2012; Shimane *et al.,* 2013). In addition, *Salinisphaera* species are also involved in the uptake of iron
447 and siderophore production (Antunes *et al.*, 2003). Molecular studies here indicated that the abundance
448 of *Salinisphaera* was consistently high in salt mats during all lake stages, except during the flooded
449 (FL) stage, where it was more abundant within the sediment. *Salinisphaera* was previously reported to

450 be the single most dominant OTU in the lake water (Zaikova *et al*., 2018) during evapo-concentration
451 in Lake Magic. These findings together indicate that most of the *Salinisphaera* spp. reside in the water
452 column of Lake Magic. The dramatic increase in its representation during the LE stage in the salt mat
453 and sediment suggests that it is highly tolerant of extreme pH and acidic environmental conditions,
454 including tolerance to heavy metal ions, allowing it to survive through the evapo-concentration stages.
455
456 Members of the *Sulfurimonas* genus have been isolated from diverse environments such as
457 hydrothermal vents, marine sediments and terrestrial habitats and are known to play an important role
458 in chemoautotrophic processes (Han and Perner, 2015). The members of this genus can grow on a
459 variety of electron donors and acceptors and, thus, are able to colonize disparate environments. These
460 include different reduced sulphur compounds such as sulphide, elemental sulphur, sulphite and
461 thiosulfate (Han and Perner, 2015). Many members of the genus are also involved in nitrogen and
462 hydrogen metabolism. In our samples, *Sulfurimonas* (1.2%) abundance continuously decreased in salt
463 mats but increased in abundance within the sediments as the environmental conditions became more
464 stressful. Ultimately, it decreased significantly during the most extreme (LE) lake stages but still
465 maintained a low representation in the sediment. When examining the functional profile data, sulphur
466 respiration significantly increased in the sediment samples during the evapo-concentration stages,
467 suggesting that *Sulfurimonas* spp play a crucial role in cycling key nutrients in the sediment. Since the
468 members of the genus are able to survive chemolithoautotrophically using various electron acceptors
469 and donors (Campbell *et al.,* 2006; Grote *et al.,* 2008), it suggests that these species are capable of
470 adapting to the changing environmental conditions of Lake Magic. A similar trend of abundance was
471 seen for *Flavobacterium, Bacillus and Syntrophobacter* genera where their abundances increased in
472 the sediment during the evapo-concentration stages and we postulate that they play a crucial role in
473 niche construction by interacting with other dominant taxa as the stress increases.

The fungal diversity was seen to decrease as the environmental conditions became more extreme. A single phylum, Ascomycota (76.8%) became dominant as the lake became dry and hypersaline. Most of the members of this phylum are unidentified, and hence, most of the fungi residing in Lake Magic are either novel, or the sequence length of the marker gene used in this study is not sufficient to be able to characterise these members. It can be deduced that these fungi are tolerant of the acidic hypersaline conditions of the lake. In a previous study on Lake Magic microbiology, the water samples were found to be highly diverse in terms of eukaryotic community composition, being abundant (~98.5%) in Ascomycota. *Aspergillus* and *Penicillium* were the most abundant genera in Lake Magic water. However, the results for sediment samples were quite similar to our results (Zaikova *et al.*, 2018). The presence of the halotolerant algae *Dunaleilla* during evapo-concentration stages is a major contributor to carbon content in the lake. It can be deduced from the data that as *Dunaleilla* increase in the Lake (during ME) the diversity in the salt mat increases rapidly. Interestingly, this difference in the diversity of lake water and sediment column indicates the exchange between the two compartments in terms of nutrition. The water column is more abundant in oxygen and has access to sunlight whilst, the higher composition of eukaryotes in the water column which contribute to the carbon and nitrogen content in the salt mat and the sediment.

In conclusion, our results highlight that the diversity in Lake Magic is strongly driven by the pH and salt concentrations at different stages of the lake. In both the salt mat and sediment samples, bacteria were found to be more abundant in the lake, comprising of halotolerant and acidotolerant species and only a small representation of archaea was seen. We can conclude from our results that, the sediment was seen to become more specialised in microorganisms involved in buffering their external environment, evident from the increase in abundance of acidotolerant and halotolerant species involved in various functions such as sulphur and iron metabolism. Moreover, due to microbial activity the environmental conditions do not change to the same degree in the sediment when compared to the salt

499 mat, resulting in a safe haven for microbes, where they are able to thrive during extreme conditions.
500 These findings confirm our hypothesis that during stressed conditions, microorganisms extensively
501 rely on associations with other microorganisms and the interactions increasingly become positive
502 (Piccardi *et al.,* 2019). This also suggests that microbial interactions are involved in stabilising the
503 ecosystem and is responsible for the resistance and resilience of these communities (Zengler and
504 Zaramela, 2018; Naidoo *et al.*, 2019).
505

References

Aerts JW, van Spanning RJM, Flahaut J, Molenaar D, Bland PA, Ehrenfreund P, Martins Z (2019). Microbial Communities in Sediments From Four Mildly Acidic Ephemeral Salt Lakes in the Yilgarn Craton (Australia) – Terrestrial Analogs to Ancient Mars. Front Microbiol;10:779.

Antunes A, Eder W, Fareleira P, Santos H, Huber R (2003). Salinisphaera shabanensis gen. nov., sp. nov., a novel, moderately halophilic bacterium from the brine-seawater interface of the Shaban Deep, Red Sea. Extremophiles; 7(1):29-34.

Antunes A, Ngugi DK, Stingl U (2011). Microbiology of the Red Sea (and other) deep-sea anoxic brine lakes. Environ Microbiol Rep; 3(4):416–33.

Bae GD, Hwang CY, Kim HM, Cho BC (2010). Salinisphaera dokdonensis sp. nov., isolated from surface seawater. Int J Syst Evol Microbiol; 60(3):680–5.

Benison KC, Beitler Bowen B, Oboh-Ikuenobe FE, Jagniecki EA, Laclair DA, Story SL, Melanie RM, Hong B-Y (2007). Sedimentology of acid saline lakes in Southern Western Australia: newly described processes and products of an extreme environment. J Sediment Res; 77:366–88.

Benison KC, Bowen BB (2006). Acid saline lake systems give clues about past environments and the search for life on Mars. Icarus; 183(1):225–9.

Bowen BB, Benison KC (2009). Geochemical characteristics of naturally acid and alkaline saline lakes in southern Western Australia. Appl Geochemistry 24(2):268–84.

Bray JR, Curtis JT (1957). An Ordination of the Upland Forest Communities of Southern Wisconsin. Ecol Monogr; 27(4):325–49.

Campbell BJ, Engel AS, Porter ML, Takai K (2006). The versatile ε-proteobacteria: Key players in sulphidic habitats. Nature Reviews Microbiology; 4: 458–68.

Caporaso JG, Kuczynski J, Stombaugh J, Bittinger K, Bushman FD, Costello EK, Fierer N, Pena, AG, Goodrich, JK, Gordon, JI, Huttley, GA (2010). QIIME allows analysis of high-throughput community sequencing data. Nat Methods; 7(5): 335.

ChénardCh C, Wijaya W, Vaulot D, Lopes dos Santos A, Martin P, Kaur A, Federico L (2019). Temporal dynamics of Bacteria, Archaea and protists in equatorial coastal waters. bioRxiv; 658278.

Conner AJ, Benison KC (2013). Acidophilic Halophilic Microorganisms in Fluid Inclusions in Halite from Lake Magic, Western Australia. Astrobiology13(9):850–60.

Crespo-Medina M, Chatziefthimiou A, Cruz-Matos R, Pérez-Rodríguez I, Barkay T, Lutz RA, Starovoytov V, Vetriani C (2009). Salinisphaera hydrothermalis sp. nov., a mesophilic, halotolerant, facultatively autotrophic, thiosulfate-oxidizing gammaproteobacterium from deep-sea hydrothermal vents, and emended description of the genus Salinisphaera. Int J Syst Evol Microbiol; 59(6):1497–503.

Cruaud P, Vigneron A, Fradette M-S, Dorea CC, Culley AI, Rodriguez MJ, Steve J (2019). Annual Protist Community Dynamics in a Freshwater Ecosystem Undergoing Contrasted Climatic Conditions: The Saint-Charles River (Canada). Front Microbiol; 10: 2359.

Darling AE, Jospin G, Lowe E, Matsen FA, Bik HM, Eisen JA (2014). PhyloSift: phylogenetic analysis of genomes and metagenomes. PeerJ; 2:e243.

Dixon P (2003). VEGAN, a package of R functions for community ecology. J Veg Sci; 14:927–30.

Dopson M, Holmes DS, Lazcano M, McCredden TJ, Bryan CG, Mulroney KT, et al (2017). Multiple Osmotic Stress Responses in Acidihalobacter prosperus Result in Tolerance to Chloride Ions. Front Microbiol 7:2132.

Dyall-Smith, M. (2009) 'The Halohandbook. Protocols for haloarchaeal genetics', version 7.2.

Elser JJ, Bracken MES, Cleland EE, Gruner DS, Harpole WS, Hillebrand H, Jacqueline TN, Eric WS, Jonathan BS, Jennifer ES (2007). Global analysis of nitrogen and phosphorus limitation of primary producers in freshwater, marine and terrestrial ecosystems. Ecol Lett; 10(12):1135–42.

Gi DB, Chung YH, Hye MK, Byung CC (2010). Salinisphaera dokdonensis sp. nov., isolated from surface seawater. Int J Syst Evol Microbiol; 60(3):680–5.

Grote J, Jost G, Labrenz M, Herndl GJ, Jürgens K (2008). Epsilonproteobacteria represent the major portion of chemoautotrophic bacteria in sulfidic waters of pelagic redoxclines of the baltic and black seas. Appl Environ Microbiol; 74(24):7546–51.

Han Y, Perner M (2015). The globally widespread genus Sulfurimonas: versatile energy metabolisms and adaptations to redox clines. Front Microbiol; 6:989.

Heidelberg KB, Nelson WC, Holm JB, Eisenkolb N, Andrade K, Emerson JB (2013). Characterization of eukaryotic microbial diversity in hypersaline Lake Tyrrell, Australia. Front Microbiol 4:115.

Johnson SS, Chevrette MG, Ehlmann BL, Benison KC (2015). Insights from the metagenome of an acid salt lake: the role of biology in an extreme depositional environment. PLoS One 10(4):e0122869.

Ju F, Zhang T (2014). Bacterial assembly and temporal dynamics in activated sludge of a full-scale municipal wastewater treatment plant. ISME J;9(3):683.

564 Louca S, Parfrey LW, Doebeli M (2016). Decoupling function and taxonomy in the global ocean microbiome. Science
565 ;353(6305):1272–7.
566 Lu S, Gischkat S, Reiche M, Akob DM, Hallberg KB, Küsel K (2010). Ecophysiology of Fe-cycling bacteria in acidic
567 sediments. Appl Environ Microbiol; 76(24):8174–83.
568 Lu S, Peiffer S, Lazar CS, Oldham C, Neu TR, Ciobota V, Nab O, Lillicrap A, Rosch P, Popp J, Kusel K (2016).
569 Extremophile microbiomes in acidic and hypersaline river sediments of Western Australia. Environ Microbiol Rep;
570 8(1):58–67.
571 Mormile MR, Hong B, Adams NT, Benison KC, Oboh-Ikuenobe F. Characterization of a moderately halo-acidophilic
572 bacterium isolated from Lake Brown, western Australia (2007). International Society for Optics and Photonics;
573 66940X.
574 Mormile MR, Hong B-Y, Benison KC (2009). Molecular Analysis of the Microbial Communities of Mars Analog Lakes
575 in Western Australia. Astrobiology ;9(10):919–30.
576 Naidoo RK, Simpson ZF, Oosthuizen JR, Bauer FF (2019). Nutrient Exchange of Carbon and Nitrogen Promotes the
577 Formation of Stable Mutualisms Between Chlorella sorokiniana and Saccharomyces cerevisiae Under Engineered
578 Synthetic Growth Conditions. Front Microbiol;10:609.
579 Nagarkar M, Countway PD, Du Yoo Y, Daniels E, Poulton NJ, Palenik B (2018). Temporal dynamics of eukaryotic
580 microbial diversity at a coastal Pacific site. ISME J;12(9):2278–91.
581 Park S-J, Cha I-T, Kim S-J, Shin K-S, Hong Y, Roh D-H, Sung K-R (2012). Salinisphaera orenii sp. nov., isolated from a
582 solar saltern. Int J Syst Evol Microbiol; 62(8):1877–83.
583 Piccardi P, Vessman B, Mitri S (2019). Toxicity drives facilitation between 4 bacterial species. Proc Natl Acad Sci USA;
584 116(32):15979-1584.
585 Podell S, Emerson JB, Jones CM, Ugalde JA, Welch S, Heidelberg KB, Banfield JF, Aleen EE (2014). Seasonal fluctuations
586 in ionic concentrations drive microbial succession in a hypersaline lake community. ISME J; 8(5):979–90.
587 Quast C, Pruesse E, Yilmaz P, Gerken J, Schweer T, Yarza P, Peplies J, Glockner FO (2012). The SILVA ribosomal RNA
588 gene database project: improved data processing and web-based tools. Nucleic Acids Res; 41(D1):D590–6.
589 R Core Team (2014). R: A language and environment for statistical computing. R Foundation for Statistical Computing,
590 Vienna, Austria.
591 Ruecker A, Schröder C, Byrne J, Weigold P, Behrens S, Kappler A (2016). Geochemistry and Mineralogy of Western
592 Australian Salt Lake Sediments: Implications for Meridiani Planum on Mars. Astrobiology;16(7):525–38.

Sánchez-Andrea I, Rodríguez N, Amils R, Sanz JL (2011). Microbial diversity in anaerobic sediments at Río Tinto, a naturally acidic environment with a high heavy metal content. Appl Environ Microbiol; 77(17):6085–93.

Sherwood JE, Stagnitti F, Kokkinn MJ, Williams WD (1991). Dissolved oxygen concentrations in hypersaline waters. Limnol Oceanogr; 36(2):235–50.

Shiers DW, Blight KR, Ralph DE (2005). Sodium sulphate and sodium chloride effects on batch culture of iron oxidising bacteria. Hydrometallurgy; 80(1–2):75–82.

Shimane Y, Tsuruwaka Y, Miyazaki M, Mori K, Minegishi H, Echigo A, Ohta Y, Maruyama T, Grant WD, Hatada Y (2013). Salinisphaera japonica sp. nov., a moderately halophilic bacterium isolated from the surface of a deep-sea fish, Malacocottus gibber, and emended description of the genus Salinisphaera. Int J Syst Evol Microbiol; 63(6):2180–5.

Suzuki I, Lee D, Mackay B, Harahuc L, Oh JK (1999). Effect of various ions, pH, and osmotic pressure on oxidation of elemental sulfur by Thiobacillus thiooxidans. Appl Environ Microbiol; 65(11):5163–8.

Weber KA, Achenbach LA, Coates JD (2006). Microorganisms pumping iron: Anaerobic microbial iron oxidation and reduction. Nature Reviews Microbiology; 4:752–64.

Whiteley AS, Jenkins S, Waite I, Kresoje N, Payne H, Mullan B, Richard A, Anthony OD (2012). Microbial 16S rRNA Ion Tag and community metagenome sequencing using the Ion Torrent (PGM) Platform. J Microbiol Methods; 91(1):80–8.

Wickham H (2011). ggplot2. Wiley Interdiscip Rev Comput Stat; 3(2):180–5.

Yahya A, Hallberg KB, Johnson DB (2008). Iron and carbon metabolism by a mineral-oxidizing Alicyclobacillus-like bacterium. Arch Microbiol; 189(4):305–12.

Zaikova E, Benison KC, Mormile MR, Johnson SS (2018). Microbial communities and their predicted metabolic functions in a desiccating acid salt lake. Extremophiles, 22(3):367–79.

Zengler K, Zaramela LS (2018). The social network of microorganisms — how auxotrophies shape complex communities. Nat Rev Microbiol; 16(6):383–90.

Zhang YJ, Tang SK, Shi R, Klenk HP, Chen C, Yang LL, Zhou Y, Li WJ (2012). Salinisphaera halophila sp. nov., a moderately halophilic bacterium isolated from brine of a salt well. Int J Syst Evol Microbiol; 62(9):2174–9.

Figure legends

Figure 1: A single core of sample (~6 cm long) showing the salt mat and sediment sections. The bottom figure shows the salt mat with salt crystals on the top of sediment, sampled as a separate sample**.**

Figure 2: Five stages of Lake Magic in a span of one-year (a) July 2017, flooded (b) October 2017, early evapo-concentration (c) January 2018, mid evapo-concentration (d) March 2018, late evapo-concentration (e) July 2018, early flooding.

Figure 3: (a) 16S rRNA gene OTU richness (ANOVA, p= 0.001) and (b) Shannon diversity index (ANOVA, p<0.001) at phylum level. The letters show significant differences as obtained with Tuckey post hoc test. Colours represent: Sediment Salt mat. FL EE ME. LE EF

Figure 4: (a) ITS gene OTU richness (ANOVA, p= 0.001) and (b) Shannon diversity index (ANOVA, p<0.001) at phylum level. The letters show significant differences as obtained with *Tuckey post hoc* test. Colours represent: Sediment Salt mat FL EE ME LE EF

Figure 5: Beta diversity of (A) 16S rRNA (B) ITS sequences for different time points and layers. Samples are coloured according to the time points and shaped according to the layer

Figure 6: Dot plot showing the FAPROTAX predicted functions of the bacterial community within the salt mat and sediment samples at different lake stages.

Sample code	Date collected	Lake stage	pH	EC	Temperature (°C)	Lake description
FL	**July 2017**	Flooded	4.5* 4.2^	7* 73.5^	16	Clear blue lake water, very thin salt mat layer
EE	**October 2017**	Early evapo-concentration	4.5* 4.1^	11.3* 78.3^	25	Shallow blue water, salt mat becomes more evident
ME	**January 2018**	Mid evapo-concentration	4.5* 3.4^	15.95* 146.9^	28	Yellow slime water, salt foams forms on the lakeshore, thick salt mat layer develops, strong pungent smell in the air
LE	**March 2018**	Late evapo-concentration	4.2* 2.7^	41.8* 223.8^	33	A thick layer of salt mat with visible halite precipitation as crystals
EF	**July 2018**	Early flooding	4.8* 3.41^	55.9* 226.7^	24	Salt mat intact, water fills the dry lake bed, clear blue water

647 **Table 1:** Description of sampling site at different sampling time points (* sediment, ^ lake water), (EC calculate in mS/cm)

648

649

Stage	Sampling time	% Carbon	% Nitrogen	Al (mg/kg)	B (mg/kg)	Ca (mg/kg)	Cu (mg/kg)	Fe (mg/kg)	K (mg/kg)	Mg (mg/kg)	Mn (mg/kg)	Na (mg/kg)	P (mg/kg)	S (mg/kg)	Zn (mg/kg)
Early flooding	**July 2018**	1.56	0.064	1186	6.8	10790	0.7	33	781	2661	1.5	33759	7.4	9190	0.2
Late evapo-concentration	**March 2018**	0.739	0.085	1099	7.5	20565	0.6	77	1065	2750	2.5	37861	8	16261	0.2
Mid evapo-concentration	**Jan 2018**	1.30	0.088	1256	5.7	2750	0.6	52	598	1462	1.5	19260	12	2591	0.2
Early evapo-concentration	**Oct 2017**	0.597	0.061	1023	3.6	11308	0.4	47	357	733	0.9	9526	10	8716	0.1
Flooding	**July 2017**	1.01	0.062	1007	3.7	350	0.8	64	323	587	0.6	7056	6	488	0.1

650 **Table 2:** Chemical data for samples at different time points. All values shown are assessed using a single sample at each time point.
651
652

653

654

655

656

657

658

659

660

661

662

663

664

665

683

684
685

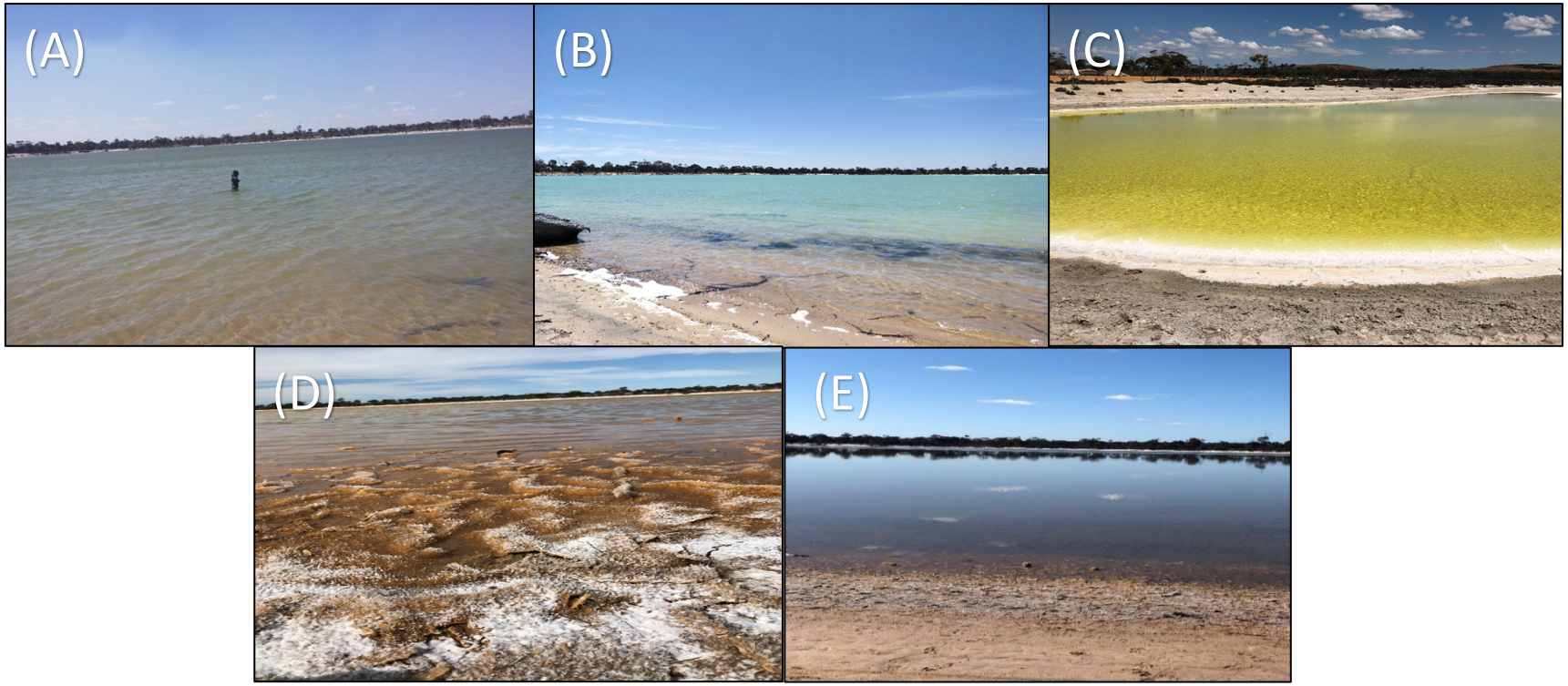
(A)
(B)
(C)
(D)
(E)

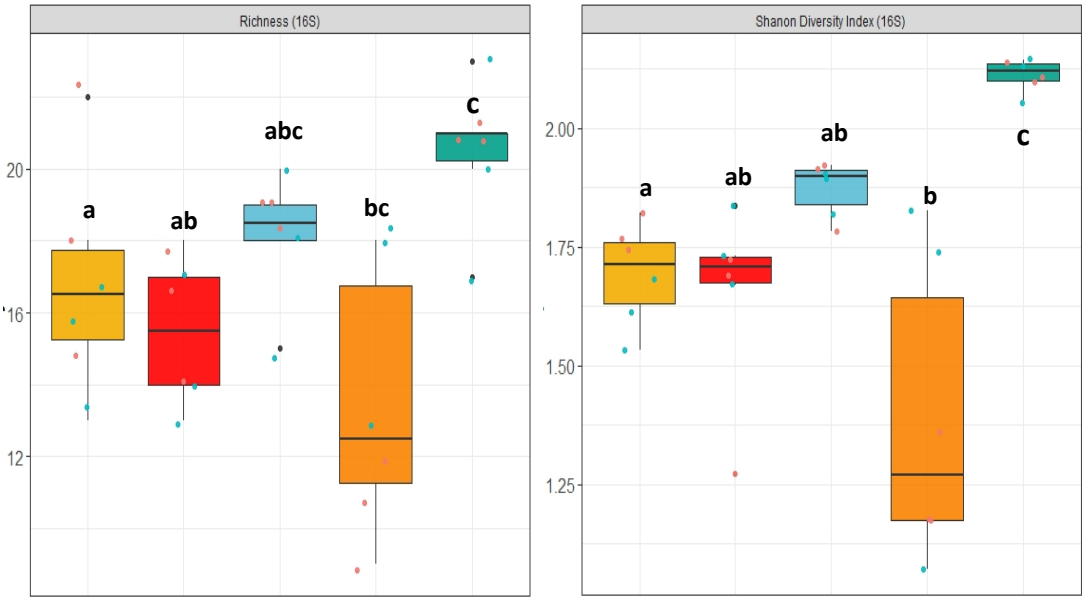

Figure 3A and 3B

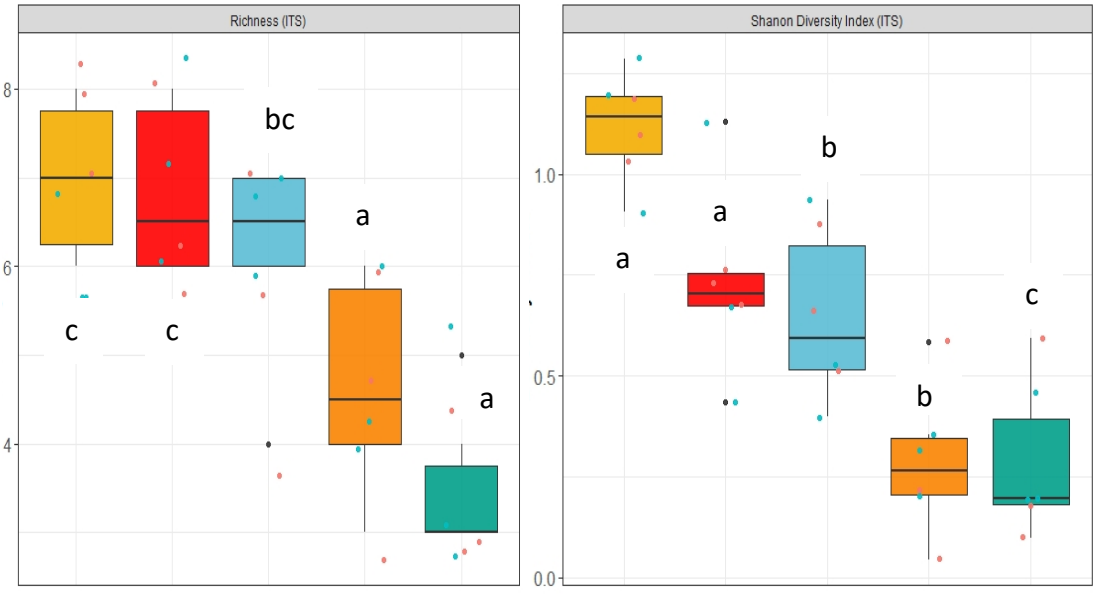

Figure 4A and 4B

Figure 5A and 5B